Reducing the positional modulation of NbO_6-octahedra in $Sr_xBa_{1-x}Nb_2O_6$ by increasing the Barium content: A single crystal neutron diffraction study at ambient temperature for $x=0.61$ and $x=0.34$

Dr. Jürg Schefer: Laboratory for Neutron Scattering, ETH Zurich & Paul Scherrer Insitute, Bldg., WHGA-244, 5232 Villigen PSI , Switzerland
Tel: +41-56-3104347, Fax: +49-56-31023191, E-Mail: jurg.schefer@psi.ch

Dr. Dominik Schaniel: I. Physikalisches Institut, Zülpicher Strasse, 77, 50937 Köln , Germany
Tel: +49-221-4706355, Fax: +49-221-4705162, E-Mail: dominik.schaniel@uni-koeln.de

Dr. Vaclav Petříček: Institute of Physics, Academy of Sciences of the Czech Republic, Na Slovance 2, 18221 Prague , Czech Republic
Tel: +420-220-318598, Fax: +420-233-343184, E-Mail: petricek@fzu.cz

PD Dr. Theo Woike: I. Physikalisches Institut, Zülpicher Strasse, 77, 50937 Köln , Germany
Tel: +49-221-4706355, Fax: +49-221-4705162, E-Mail: Th.Woike@uni-koeln.de

Dr. Alain Cousson: Laboratoire Léon Brillouin, CEA-CNRS, 91191 Gif-sur-Yvette , France
Tel: +33-169-086431, Fax: +33-169-088261, E-Mail: cousson@llb.saclay.cea.fr

PD Dr. Manfred Wöhlecke: Fachbereich Physik,University of Osnabrück, Barbarastrasse, 7, 49069 Osnabrück , Germany
Tel: +49-541-9692631, Fax: +49-541-9693512, E-Mail: manfred.woehlecke@uos.de

MS-ID:	jurg.schefer@psi.ch	July 18, 2008
Heft: / ()		

Abstract

We report on the influence of the Barium content on the modulation amplitude in $Sr_xBa_{1-x}Nb_2O_6$ compounds by comparing $Sr_{0.61}Ba_{0.39}Nb_2O_6$ (SBN61) and $Sr_{0.34}Ba_{0.66}Nb_2O_6$ (SBN34). Our single crystal neutron diffraction results demonstrate that the amplitude of the positional modulation of the NbO_6 octahedra is reduced with increasing barium content, indicating that the origin of the modulation is the partial occupation of the pentagonal channels by Sr and Ba atoms. By increasing the Sr content the bigger Ba atoms are replaced by the smaller Sr atoms, which leads to a larger deformation of the surrounding lattice and hence to a larger modulation amplitude. The more homogeneous the filling of these channels with one atomic type (Ba) the lower the modulation amplitude. Our results also show that the structure can be described with a two-dimensional incommensurate harmonic modulation. No second order modulation has been observed, both by single crystal diffraction measurements and q-scans. The positional modulation of the Nb atoms is much smaller than that of the oxygen atoms, such that the modulation can be seen as a rotational modulation of almost rigid NbO_6-octahedra.

Zusammenfassung

Wir berichten über den Einfluss des Bariumgehalts auf die modulierte Struktur von $Sr_{0.61}Ba_{0.39}Nb_2O_6$ (SBN61) und $Sr_{0.34}Ba_{0.66}Nb_2O_6$ (SBN34) bei Umgebungstemperatur. Unsere Resultate basieren auf Neutronendiffraktionsmessungen an Einkristallen und können mit einer modulierten Struktur im (3+2) Raum beschrieben werden. Unsere Resultate können wir mit zwei inkommensurablen harmonischen Modulationen beschreiben. Die Modulationsamplitude der Positionen der Nb Atome is viel kleiner als jene der Sauerstoffatome. Damit können wir die Modulation der NbO_6-Oktaeder als Rotationen von starren Körpern betrachten und mit einer harmonischen Modulation beschreiben. Weder mit Einkristallmessungen noch mit qscans konnten höherer harmonische Beiträge gefunden werden. Mit höherem Bariumgehalt wird die Modulation reduziert. Je homogener diese Kanäle mit einem Atomtyp (Ba) gefüllt sind, desto kleiner ist die Amplitude der Modulation. Wenn wir den Sr Gehalt erhöhen und die grösseren Ba Atome durch die kleineren Sr Atome ersetzen werden, erniedrigt sich die Deformation der Gitterumgebung und führt damit zu einer Reduktion der Modulationsamplitude, wie sie in unserem Experiment beobachtet wird. Dies ist ein Indiz dafür, dass die partielle Besetzung der Pentagonkanäle durch Sr und Ba Atome die Ursache der Modulation ist.

1 Introduction

The uniaxial ferroelectric relaxor Strontiumbariumniobate (SBN), $Sr_xBa_{1-x}Nb_2O_6$ $(0.26 \leq x \leq 0.87)$[1], is a photorefractive material usable in a variety of optical applications, such as optical data storage [2] and data processing [3] as well as optical phase conjugation [4]. These applications are based on the high photorefractive sensitivity. Additionally the material has large pyroelectric, electro-optic, and piezoelectric coefficients [5, 6, 7]. Furthermore, SBN is a model substance for the investigation of the relaxor type ferroelectric phase transition, where ferroelectric nanoclusters are stabilized by internal random fields above the critical temperature T_c over a wide temperature range, such that the ferroelectric polarization does not decay spontaneously at T_c [8]. This relaxor behavior is well explained by the Random-Field-Ising model for the ferroelectric phase transition. Assuming an internal random electric field, all critical exponents could be determined according to the scaling relation [9, 10, 11]. They fulfill the Rushbroke relation and belong to the universal class of the three-dimensional Random-Field-Ising model. Note however, that the model underlying the ferroelectric relaxor properties of SBN is a controversial issue, as discussed, e.g., in Ref. [12]. From a structural point of view the space group of the average structure changes from $P-4b2$ to $P4bm$ during this high-temperature ferroelectric phase transition, while the incommensurate modulation remains [13, 14].

The average structure of congruently melting $Sr_{0.61}Ba_{0.39}Nb_2O_6$ (SBN61) in the ferroelectric phase, spacegroup $P4bm$ (No. 100), has been determined by x-ray diffraction [15], showing that the structure is a three-dimensional network of NbO_6-octahedra linked at their corners forming alternating five- and four-membered rings (see Fig. 1). The structure contains two crystallographically non-equivalent Nb-atoms: Nb1 and Nb2. The Nb(1)-O_6-octahedra have point-symmetry $mm2$ and form infinite chains of the composition $[NbO_5]^{5-}$ along the crystallographic c-axis. The Nb(2)-O_6-octahedra are located in general positions (point symmetry 1) and form channels along the c-axis of square cross section. The Sr atoms occupy positions of symmetry 4 inside these square channels. This is illustrated in Fig. 1 showing the pentagonal channels A1 occupied by

Sr only and the channels A2 filled by Sr/Ba. The trigonal channels C remain empty. The pentagonal channels are wider than the square channels. All the Ba and some of the Sr atoms are located in such larger channels (point symmetry m), which are not fully occupied. Five Sr and Ba atoms are distributed over six sites. In the early structure determinations of SBN [16] split positions for Oxygen atoms were introduced to account for the disorder caused by the Sr/Ba distribution in the crystals. Later Schneck $et\ al.$ [13] observed satellite spots at positions $(h \pm \frac{1+\delta}{4}, k \pm \frac{1+\delta}{4}, l \pm \frac{1}{2})$ with $\delta = 0.26(5)$ in $Sr_{0.71}Ba_{0.29}Nb_2O_6$, which revealed the incommensurate nature of the structural modulation. These results were confirmed by Balagurov $et\ al.$ [14] in neutron time-of-flight measurements on $Sr_{0.7}Ba_{0.3}Nb_2O_6$ where $\delta = 0.22(1)$ was found. More time-of-flight studies revealed that the modulation parameter δ is slightly decreasing with decreasing Sr-concentration x for different compositions $0.46 < x < 0.75$ [17]. From electron diffraction measurements on $Sr_{0.5}Ba_{0.5}Nb_2O_6$ $\delta = 0.190(5)$ was reported [18]. Only recently x-ray measurements with a systematic collection of satellite reflections were performed on a $Sr_{0.61}Ba_{0.39}Nb_2O_6$ single crystal and subsequently analyzed in terms of the superspace formalism [19].

Recently the average structure of $Sr_xBa_{1-x}Nb_2O_6$ in the composition range $0.32 < x < 0.82$ was systematically investigated by X-ray diffraction [21]. It was shown that the lattice parameters a and c decrease with increasing strontium content, which could be ascribed to the exchange of Ba by Sr in the pentagonal A2 channels. The occupation of the square A1 channels remains nearly constant for all concentrations x. In order to explore the influence of the composition x on the modulated structure and its physical origin in SBN we present here a neutron diffraction investigation on single crystals of $Sr_xBa_{1-x}Nb_2O_6$ with the two compositions x=0.61 and x=0.34. As demonstrated in a recent powder diffraction study on SBN [22], neutron diffraction is especially suited for this kind of structural investigation, because the neutron scattering length of O (5.803 fm) is of the same order of magnitude as that of the heavy nuclei Sr (7.02 fm) and Ba (5.06 fm). Therefore the description of a positional modulation of the Oxygen atoms beside the heavy atoms Strontium and Barium is possible with high accuracy. A second reason to use neu-

tron diffraction is the fact, that neutrons are scattered by the nucleus, making them very sensitive to positional disorder as shown e.g. by many studies investigating Cu-O distances in high-temperature superconductors as successfully shown by [23]. The data are analyzed using the superspace approach for the description of the two-dimensional incommensurate modulation.

2 Experimental and Computational Details

The crystals of SBN61 and SBN34 were grown by the Czochralski method in the crystal growth laboratory of the University of Osnabrück.

For the q-scans on SBN61 on the cold triple axis spectrometer TASP [24]/SINQ[25] and the measurements on TriCS[26]/SINQ, a crystal of size $4x4x5mm^3$ was poled by applying an electric field of 500V/mm along the crystallographic c-axis during 6 hours at 23°C. The same SBN61 crystal was polarised by applying 270 V/mm at T=130°C and field-cooled down to room temperature before the full data collection on the hot neutron diffractometer 5C2/LLB (dataset 1). An additional dataset on the same SBN61 crystal has been collected at TriCS (Tab. VII-IX, appendix [27])in order to test the crystal for the 5C2/LLB measurement and to make first searches for potential second order satellites.

The SBN61 (dataset 1) crystal has an almost cubic shape with with minor crystallographic faces on the edges. The size of the unpoled crystal of SBN34 measured on TriCS/SINQ (dataset 2) is has maximum dimensions $9x9x9mm^3$ with non rectangular faces of known crystallographic orientation. All experimental conditions are listed in Table 1.

2.1 Data Collection

For the data collection, we doubled the tetragonal c-axis in order to match the later refinement with the incommensurate modulation vectors $\mathbf{Q_{1,2}}=(\alpha,\pm\alpha,\frac{1}{2})$ when using the original cell. This simple transformation with twice the c parameter of the original cell makes it possible to separate internal and external parameters

completely. It leads to an additional centering which can be characterized by one non-primitive centering vector, $(0,0,\frac{1}{2},\frac{1}{2},\frac{1}{2})$. The modulated structure satellite reflections are consequently at positions given by the modulation vectors $\mathbf{Q_{1,2}}=\alpha\cdot(\mathbf{a}^* \pm \mathbf{b}^*)$ with α=0.3075 for SBN61 and α=0.2958 for SBN34, respectively, with c = 2 $\cdot c_{av}$. Data sets were collected on the instruments 5C2/LLB (SBN61, dataset 1) and TriCS/SINQ (SBN34, dataset 2). Data collections were performed using ω-scans and single detectors for all instruments. Lorenz correction has been applied to all datasets. The measurements are summarized in Table 1. Absorption was corrected in JANA2000 [28] using the exact shape of the crystal.

The TASP/SINQ instrument was used to perform high-resolutions q-scans in order to search weak higher order satellites not detected on the single crystal diffraction instruments. TASP is especially suited for this purpose due to its very low background: High collimation and suppressing inelastic scattering increase the peak-to-background relation on this instrument dramatically in respect to conventional diffraction instruments such as 5C2 or TriCS.

2.2 Refinement

The average structure is refined in the space group $P4bm$ (No. 100). The tetragonal lattice parameters are $c = 7.8856(2)$ Å and $a = 12.4815(3)$ Å ($c = 2 \cdot c_{av}$ has been doubled). The Ba content is fixed at $1 - x = 0.39$ for SBN61 and $1 - x = 0.66$ for SBN34. These values were determined by X-ray fluorescence [1] and neutron activation [29] analysis. The sum of the occupancies of atoms Sr1, Sr2 and Ba2 was constraint to 1. The coordinates as well as the displacement parameters of the Atoms Sr2 and Ba2, sharing the same crystallographic site (4c) in channel A2 in a statistical manner, are constrained. Isotropic extinction correction Type I (Lorentz distribution of mosaics) has been applied [30, 31, 32]. For the modulated structures, the superspace group P4bm $(\alpha,\alpha,\frac{1}{2},\alpha - \alpha,\frac{1}{2})$ as tabulated by De Wolff [33] has been used. The refinement has been done in 5-dimensional superspace as described by de Wolff [33] and Janner & Janssen [34, 35] using the program JANA2000 [28]. The details of this concept for

the present case (2 modulation vectors, 5 dimensional space) are given in Refs. [19] or [36].

3 Results

Main structural results are discussed on the example of SBN61, since the peculiarities of the modulated structure are more pronounced than in SBN34. Furthermore the results can be compared to the available X-ray refinement [19]. On the other hand, the comparison to the results of the SBN34 structural analysis gives clear evidence of the origin of the modulation. In order to clarify a possible disorder of the Strontium and Barium sites and to estimate the influence of anisotropic temperature factors we have also analysed the average structure of SBN61 carefully. This procedure is necessary for a sound interpretation of the subsequent modulated refinements.

3.1 Average Structure of SBN61

The average structure has been refined using a fixed Ba content of $1 - x = 0.39$. The tetragonal lattice parameters are a=12.481(8) Å, c=7.885(6) Å (also in this case, we used $c = 2 \cdot c_{av}$ for better comparison of the results). The refinement with isotropic displacement parameters U_{iso} yields agreement factors $R = 0.195$ and Goodness of fit $S = 26.3$. The refined parameters are given in [20]. The refinement can be improved by introducing anisotropic displacement parameters U_{ij} $(i, j = 1, 2, 3)$ yielding $R = 0.093$, $S = 12.2$, at the cost of negative values for the atom Nb1 (Tables VII and X in the appendix [27]). In both cases large displacement parameters are obtained for Sr2/Ba2 and all Oxygen atoms. Sr2/Ba2, O4 and O5 exhibit large values of U_{11}, U_{22}, and U_{12} whereas for O1, O2 and O3 large values of U_{33} are obtained, indicating that the modulation of the former are within the tetragonal plane, whereas that of the latter are along the crystallographic c-direction. Refining the atoms Sr2/Ba2 unrestricted does not improve the quality of the fit and is therefore not considered for the final refinement. Looking at the difference Fourier map (Fig. 2) one can clearly see the mismatch in the refinement at the O4 and partially O5 positions for SBN61. Refining split positions for the O4 atom im-

proves the agreement factors significantly to $R = 0.063$ but at the cost of negative displacement parameters for several atoms and is therefore discarded as an unphysical solution of the structure. As is evident from the difference Fourier map (Fig. 2), one would have to introduce more than two positions to describe the behavior at the O5 position. The refinement of the average structure from neutron data is in agreement with that observed by x-rays [19], but also shows that the inclusion of a modulation as done in the next section is imperative.

3.2 Modulated Structures of SBN61 and SBN34

The analysis of the modulated structure is done using the superspace approach. Thereby the incommensurate modulation is described using a five-dimensional space, in order to account for the two modulation vectors $\mathbf{Q_{1,2}} = (\alpha, \pm\alpha, 0)$, where $\mathbf{Q_{1,2}}$ is in respect to the doubled c axis as defined in Tab. 1. The method is summarized in detail in Ref. [19, 27].

The refinements are performed in the superspace group $P4bm(\alpha\alpha\frac{1}{2}, \alpha - \alpha\frac{1}{2})$. Starting from the average structure, two harmonic positional modulation waves are introduced for all atoms. Again, the parameters of Sr2 and Ba2 located in channel A2 (see Fig. 1) are constrained to have identical positional and displacement parameters in all refinements. Introduction of an additional occupational disorder function for Sr2/Ba2 did not result in significant improvements of the agreement factors and was therefore not taken into account in the final refinement. However we introduced two modulation waves for the displacement parameters of the Sr2/Ba2 atoms in order to take into account that two different atoms occupy the same position. These two modulation waves then incorporate effects originating from the slightly varying positions of Sr2/Ba2 in the disordered lattice, e.g., different orientations of the thermal ellipsoids. The displacement parameters are chosen anisotropic, yielding minor negative values for the Oxygen atoms. The refinement for the two datasets of SBN61 collected on the instrument 5C2 (dataset 1) and TriCS (dataset 3 with lower q-range, discussed in detail in the thesis of Schaniel [20], tables summarized in the appendix [27]) are in excellent agreement. However, small residual differences remain, as e.g shown by the

5

difference Fourier maps around oxygen atoms O4 and O5 (Fig. 3), but are dramatically reduced compared to the refinement using an average structure (see Fig. 2). As illustrated in Fig. 4 similar difference Fourier maps are obtained for SBN34 after final refinement, however the remaining residuals are much smaller than in the SBN61.

The final refinement of the structure yields total agreement factors of $R_{w,obs} = 0.0908$, $S = 7.15$ and agreement factors of $R_{all} = 0.0579$ for main and $R_{w,all} = 0.192$ for satellite reflections for SBN61. For SBN34 total agreement factors of $R_{w,obs} = 0.111$, $S = 6.96$ and agreement factors of $R_{all} = 0.091$ for main and $R_{w,all} = 0.134$ for satellite reflections are obtained. This is approximately a factor of two above the agreement factors obtained from the extended X-ray data sets of SBN61 collected by Woike et al. [19] yielding a R_w of 0.045 for the main reflections and R_w of 0.126 for the satellite reflections. This indicates that the positions of the oxygen could have a systematic error, as neutrons are more sensitive to the oxygen positions compared to X-ray diffraction studies. Note however that the X-ray study on SBN61 was performed only up to $\sin\theta/\lambda$-values of $0.75\,\text{Å}^{-1}$, while our neutron study goes up to $1.0\,\text{Å}^{-1}$.

The full parameter set of the final refinement are available from the supplementary material [27]. It can be seen that the form of the modulation is the same for SBN61 and SBN34, but the amplitude is reduced by a factor of two in SBN34. A comparison between selected values is listed in Table 4. The sine- and co-sine part of the harmonic modulation waves belonging to the two modulation vectors are indicated by s, m, n and $c, m, n(m, n = 0, 1)$, e.g. $s, 1, 0$ is the sinusoidal modulation contribution from the modulation vector $\mathbf{Q_1}$. Overall the atoms Sr2/Ba2, O4, and O5 are modu-lated in the tetragonal ab-plane whereas the atoms O1, O2, and O3 are mainly modulated along the c-direction of the crystal. The atoms Nb1, Nb2, and Sr1 exhibit only a small positional modulation. Taking exemplarily the atom O4 (which has the highest modulation am-plitude) for comparison of SBN61 and SBN34, we find that the s,1,0 amplitudes are reduced by a factor of 3 and the c,1,0 amplitudes by a factor of 2. This differ-ence in modulation amplitude is then also reflected in the minimal/maximal distances (selected values listed in Tab. 4, full listing see Tables III/IV and VII/VII

of the supplementary material [27]), where for Nb2-O4 min/max distances of $1.721(14)\,\text{Å}/2.029(15)\,\text{Å}$ and $1.746(19)\,\text{Å}/2.010(19)\,\text{Å}$ are found for SBN61 and SBN34, respectively. For Nb2-O4^{iv} the differ-ence is even more pronounced with distances of $1.959(14)\,\text{Å}/2.213(15)\,\text{Å}$ and $2.022(19)\,\text{Å}/2.280(19)\,\text{Å}$ for SBN61 and SBN34, respectively. In both cases the average distances, $1.889(15)\,\text{Å}/1.87(2)\,\text{Å}$ for Nb2-O4 and $2.109(15)\,\text{Å}/2.13(2)\,\text{Å}$ for Nb2-O4^{iv}, are the same within experimental error for SBN61 and SBN34. Com-pared to the results of the X-ray study for SBN61[19], where the interatomic distances Nb2-O5 and Nb2-O5^{iv} (O4 and O5 are interchanged in the two papers) range from $1.79(3)\,\text{Å}$ to $1.98(3)\,\text{Å}$, our study shows values between $1.95(3)\,\text{Å}$ and $2.18(3)\,\text{Å}$. Hence the modu-lation of the Nb2-O4/O4^{iv} distances in SBN61 of $0.30(3)\,\text{Å}/0.25(3)\,\text{Å}$ in the neutron case is significantly larger than the $0.19(6)\,\text{Å}/0.23(6)\,\text{Å}$ found in the X-ray study. This fact is also nicely observed in the Fourier maps, as shown for the observed positional modulation of O4, together with the fitted position along the first modulation vector $\mathbf{Q_1}$ in SBN61 in Fig. 5, which shows the larger modulation amplitude compared to the corre-sponding figure in the X-ray study (Fig. 6 in Ref. [19]). From these figures it becomes also clear why the agree-ment factors in the neutron case are worse than in the X-ray case, although the description of the O4 modula-tion seems slightly better: the high oxygen sensitivity of the neutron yields high R-values even for small mis-matches in the modulation description. In SBN34, as illustrated in Fig. 6, the modulation amplitude is sig-nificantly reduced as discussed above, leading to better agreement factors.

Similar observations concerning average, minimal, and maximal values of distances are made for the Sr/Ba-polyhedra, where in the neutron refinement a larger am-plitude is found than in the X-ray refinement, especially for the distances including the atoms O4 and O5. Here again the Sr/Ba atoms have a much smaller modula-tion amplitude than the oxygen atoms, as illustrated exemplarily for SBN61 in Fig. 7, which shows how the x-coordinate is changing as a function of t_1 for atoms Ba2, Sr1, Nb1, Nb2, ad O4, where x is defined as

$$x = x_o +$$

$$U_{xs,1,0} \cdot sin(2\pi \cdot \mathbf{Q_1} \cdot \mathbf{r_0} + t_1) +$$
$$U_{xc,1,0} \cdot cos(2\pi \cdot \mathbf{Q_1} \cdot \mathbf{r_0} + t_1) +$$
$$U_{xs,0,1} \cdot sin(2\pi \cdot \mathbf{Q_2} \cdot \mathbf{r_0} + t_2) +$$
$$U_{xc,0,1} \cdot cos(2\pi \cdot \mathbf{Q_2} \cdot \mathbf{r_0} + t_2)$$

, where $U_{yz,m,n}$ are the modulation amplitudes listed in Tab. 2.

This means, for $t_2 = 0$ the third and fourth term make just a constant but generally non-zero contribution to the curves shown in Fig. 7 for SBN61 and Fig. 8 for SBN 34, respectively. The Sr1 atoms in the tetragonal A1 channels are hardly modulated as shown in Fig. 9. Corresponding modulations in SBN34 are drastically reduced (Fig. 8). Detailed interatomic distances and full tables are listed in the supplementary material [27].

It is known from x-ray diffraction experiments on the average structure, that the occupation of the square channels (Sr1) is hardly affected by the decreasing Sr content [21]. The exchange of Sr and Ba takes place in the pentagonal channels. So for the SBN61 the site occupancies (in comparison to the the maximum occupancy of 1) are 0.72 for Sr on A1 (2a), 0.4875 for Ba on A2 (4c), and 0.402 for Sr on A2 while for SBN34 the corresponding site occupancies are 0.62 for Sr on A1, 0.825 for Ba on A2, and 0.11 for Sr on A2 [21]. Therefore in SBN34 we have an almost uni-atomic occupancy of the two sites, the A1 channels are solely occupied by Sr while on the A2 sites the Sr:Ba ratio is 1:7 compared to 6:5 in SBN61. Hence we can argue that the reduced amplitude of the modulation is due to the reduced distortion exerted on the lattice by the more homogeneous filling ratio by only one atomic type (Ba) of the A2 channels in SBN34. The modulation does not disappear due to the fact that still one of six sites remains empty.

Both, triple-axis experiments (q-scans on TASP/SINQ, Fig. 10) and measurements on the single crystal instruments 5C2/LLB (test of 829 2nd-order satellites) and TriCS (150 2nd-order satellites) showed no evidence for higher order satellites in SBN61. Therefore only harmonic modulation waves have been introduced for our refinement. There is obviously no satellite observed for positions $d_{1,2} = 2$ in Fig. 10. The observed side reflections of the satellites (0.3075,5.3075,-1) and (0.3075,5.3075,1) correspond to (002)- and (111)-aluminum-powder lines from the sample holder.

4   Conclusions

The structures of $Sr_xBa_{1-x}Nb_2O_6$, x=0.61 and 0.34, at ambient temperature can be described with two incommensurate modulations vectors $\mathbf{Q_{1,2}}$=(α,$\pm\alpha$,0) (α=0.3075 for SBN61 and α=0.2958 for SBN34) in a harmonic approximation. Our study clearly shows, that the modulation amplitude of the oxygen O4 atoms is decreasing by a factor of 2 going from SBN61 to SBN34 (increased Ba content), but has the modulation has the same shape. The positional modulation of the Nb atoms is much smaller than that of the oxygen atoms. It is is therefore originating mainly from a rotational modulation of the NbO_6-octahedra. The physical origin for this rotational modulation is most probably the filling of the pentagonal A2 channels by Sr and Ba atoms, as evidenced by the decrease of the modulation amplitude with increasing Ba content when going from SBN61 to SBN34. Due to their different size the surrounding lattice is deformed leading to the modulation of the oxygen atoms. The atom with the highest modulation is the apical O4 atom, which is in the same plane as the Sr/Ba atoms. The second type of NbO_6 octahedra is significantly less influenced by the modulation, as seen by the lower modulation amplitude of O5 (Nb(2)-O_6-octahedra) compared to O4 (Nb(1)-O_6-octahedra). Remaining intensities in the difference fourier maps around O4/O5 as well as slightly negative temperature factors show, that the model needs further improvement. However, without observing higher order satellites refinement has to stay in the harmonic approximation. From our diffraction data and extended q-scans, we can exclude satellites of second order, such as $2 \cdot \mathbf{Q_1}$, $2 \cdot \mathbf{Q_2}$, $\mathbf{Q_1} + \mathbf{Q_2}$, $\mathbf{Q_1} - \mathbf{Q_2}$. Also extended q-scans did not show any higher order satellites.

5   Acknowledgment

References

[1] Ulex, M.; Pankrath, R.; Betzler, K.: Growth of strontium barium niobate: the liquidussolidus phase diagram. *J. Cryst. Growth* 271, 2004, S. 128–133

[2] Ford, J.E.; Ma, J.; Fainman, Y.; Lee, S.H.; Yaketomi, Y.; Bize, D.; Neurganonkar, R.R.: Multiplex holography in strontium barium niobate with apllied field. *J. Opt Soc. Am.* 9, 1992, S.1183-1192

[3] Yeh, J.; Chiou, A.E.T.: Optical matrix-vector multiplication through four-wave mixing photorefractive media. *Opt. Lett.* 12, 1987, 138-140

[4] Wood, G.L.; Clark III, W.W.; Miller, M.J.; Sharp, E.J.; Salamo, G.J.; Neurgaonkar,; R.R.: Broadband photorefractive properties and self-pumped phase conjugation in Ce-SBN: 60. *IEEE J. Quant. Electron.* 23, 1987, S. 2126-2135.

[5] Ewbanks ,M. ;Neurgaonka ,R. ;Cory , W., Photorefractive properties of strontium-barium niobate. *J.Appl. Phys.*62, 1987, S. 374-380

[6] Lines ,M.E. ; Glass, A.M.: Principles and Applications of Ferroelectrics and Related Magterials. Oxford Classics Series. 2001

[7] Neurgaonkar, R.R. ; Cory , R.R. ; Oliver, R.R. ; Ewbank , R.R. ; Hall, M.E.: Development and modifiction of photorefractive properties in the tungsten bronze family crystals. *Opt.Eng.* 26, 1987, S. 392-405

[8] Bhalla, A. S.; Guo,R.; Cross,L. E.; Burns,G.; Dacol,F. H.; Neurgaonkar,R. R.: Measurements of strain and the optical indices in the ferroelectric $Ba_{0.4}Sr_{0.6}Nb_2O_6$: Polarization effects. *Phys. Rev. B* 36, 1987, S. 2030-2035

[9] Dec, J.; Kleemann, W.; Bobnar, V.; Kutnjak, Z.; Levstik, A.; Pirc, R.; Pankrath, R.: Random-field Ising-type transition of pure and doped SBN from the relaxor into the ferroelectric state. *Europhys. Lett.* 55, 2001, S. 781-787

[10] Granzow, T.; Woike, T.; Wohlecke, M.; Imlau, M.; Kleemann,W.: Change from 3D-Ising to random field-ising-model criticality in a uniaxial relaxor ferroelectric. *Phys. Rev. Lett* 92, 2004, S. 065701-1-4

[11] Kleemann, W.: The relaxor enigma - charge disorder and random fields in ferroelectrics *J. Mat. Science* 41, 2006, S. 129-136

[12] Scott, J. F.: Absence of true critical exponents in relaxor ferroelectrics: the case for defect dynamics. *J. Phys. Cond. Mat.* 18, 2006, 7123-7134

[13] Schneck, J. ; Toledano, J. ; Whatmore, R. ; Ainger, F.: Incommensurate phases in ferroelectric tetragonal tungston bronzes. *Ferroelectrics* 36, 1981, S. 327-330

[14] Balagurov, A.; Prokert, F.; Savenko, B.: Phase transition effects in the incommensurate modulated single cyrstal of $Ba_{0.3}Sr_{0.7}Nb_2O_6$ *phys. stat. sol.* 103, 1987, S. 131-144

[15] Chernaya, T.S.; Maksimov, B.A.; Verin, I.V.; Ivleva, L.I.; Simonov, V.I.: Crystal structure of $Ba_{0.39}Sr_{0.61}Nb_2O_6$ single crystals. *Cryst. Rep.* 42, 1997, S. 375-380

[16] Jamieson, P.B.; Abrahams, S.C.; Bernstein, J.L.: Ferroelectric Tungsten Bronze-type crystal structures. I. Barium Strontium Niobate $Ba_{0.27}Sr_{0.7}Nb_3O_{5.78}$. *J. Chem. Phys.* 48, 1968, S. 5048-5057

[17] Prokert, F. ; Sangaa, D. ; Savenko, B.N.: Neutron-diffraction study of the electric-field influence on $Sr_xBa_{1-x}Nb_2O_6$ mixed-crystals. *Ferroelectrics Lett.* 13, 1991, S. 61-66

[18] Bursill, L.A.; Lin, P.J.: Incommensurate superstructures and phase transition of strontium barium niobate (SBN). *Acta. Cryst. B* 43, 1987, S. 49-56

[19] Woike, T.; Petříček, V.; Dusek, M.; Hansen, N.; Fertey, P.; Lecomte, C.; Arakcheeva, A.;Chapuis, G.; Imlau, M.; Pankrath,R.: The modulated structure of $Ba_{0.39}Sr_{0.61}Nb_2O_6$. I. Harmonic solution. *Acta Cryst. B* 59, 2003, S. 28-35

[20] Schaniel, D.: Structural Investigations of High-Knowledge Content Materials. *Thesis No. 14902, ETH Zurich*, ,http://e-collection.ethbib.ethz.ch/cgi-bin/show.pl?type=diss&nr=14902, 2003

[21] Podlozhenov, S.; Graetsch, H.A.; Schneider, J.; Ulex, M.; Wöhlecke, M.: Crystal structure of strontium barium niobate $Sr_xBa_{1-x}Nb_2O_6$. *Acta Cryst. B* 62, 2006, S. 960-965

[22] Schefer, J.; Schaniel, D.; Pomjakushin, V.; Stuhr, U.; Petříček, V.; Woike, Th.; Wöhlecke, M.; Imlau,M.: Structural properties of $Sr_{0.61}Ba_{0.39}Nb_2O_6$ in the temperature range 10500 K investigated by high-resolution neutron powder diffraction and specific heat measurements. *Phys. Rev. B* 74, 2006, S. 134103-1-9

[23] Hewat, A.W.; Fischer,P.; Kaldis, E.; Karpinski, J.; Rusiecki, S.; Jilek, E.: High resolution neutron powder diffraction investigation of temperature and pressure effects on the structure of the high-Tc superconductor $Y_2Ba_4Cu_7O_{15}$. *Physica C: Superconductivity* 167, 1990, 579-590

[24] Semadeni, F.; Böni, P.; Rössli, B.: Three-axis spectroscopy with remanent benders. *Physica B* 297, 2001, S. 152-154

[25] Fischer, W.E.: SINQ - The spallation neutron source, a new research facility at PSI. *Physica B* 234-236, 1202 (1997) 1202-1208

[26] Schefer, J.; Könnecke, M.; Murasik, A.; Czopnik, A.; Strässle, T.; Keller, P.; Schlumpf, N.: Single-crystal diffraction instrument TriCS at SINQ. *Physica B*. 276-278, 2000, S. 168-169

[27] Schefer, J.; Schaniel, D. ; Petříček,V. ; Woike, Th.; Cousson, A.; Wöhlecke, M.: Full tables: Supplemenatry material for $Sr_xBa_{1-x}Nb_2O_6$, 2007

[28] Petříček, V.; Dušek, M.; Palatinus, L.: The crystallographic computing system JANA2000. *Institute of Physics*, Praha, 2000

[29] Woike, T.; Weckwerth, G.; Palme, H.; Pankrath, R.: Instrumental neutron activation and absorption spectroscopy of photrefractive strontium-niobate single crystals doped with cerium. *Solid State Commun.* 102, 1997, S. 743-747

[30] Becker, P.J.; Coppens, P.: Extinction within the limit of validity of the Darwin transfer equations. I. General formalism for primary and secondary extinction and their applications to spherical crystals. *Acta. Cryst. A* 30, 1974, S. 129-147

[31] Becker, P.J.; Coppens, P.: Extinction within the limit of validity of the Darwin transfer equations. II. Refinement of extinction in spherical crystals of SrF_2 and LiF *Acta. Cryst. A* 30, 1974, S. 148-153

[32] Becker, P.J. ; Coppens, P.: Extinction within the limit of validity of the Darwin transfer equations. III. Non spherical crystals and anisotropy of extinction. *Acta. Cryst. A* 31, 1975, S. 417-425

[33] Wolff, P.; Janssen, T.; Janner, A.: The superspace groups for incommensurate crystal structures with a one-dimensional modulation. *Acta. Cryst. A* 37, 1981, S. 625-636

[34] Janner, A.; Janssen, T.: Symmetry of incommensurate crystal phases. I. Commensurate basic structures. *Acta. Cryst. A* 37, 1980, S. 399-408

[35] Janner, A.; Janssen, T.: Symmetry of incommensurate crystal phases. II. Incommensurate basic structure. *Acta. Cryst. A* 36, 1980, S. 408-415

[36] Schaniel, D., Schefer, J.; Petříček, Imlau, M.; Granzow, T.; Woike, Th.: Superspace approach applied to a neutron-diffraction study of the holographic data storage material $Sr_{0.61}Ba_{0.39}Nb_2O_6$. *Appl. Phys. A: Mater. Sci. Process.* 74, 2002, S. S963-S965
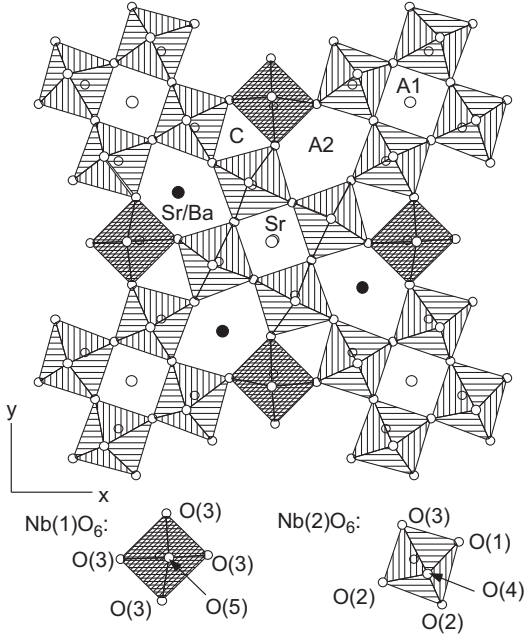
Figure 1: Projection of $Sr_{0.61}Ba_{0.39}Nb_2O_6$ along the c-axis. The pentagonal channels A2 are filled by Strontium and Barium (Sr2/Ba1), the tetragonal channels A1 by Strontium (Sr1) only, and the trigonal channels C remain empty. 5 Sr/Ba atoms are distributed over 6 A1/A2 sites.
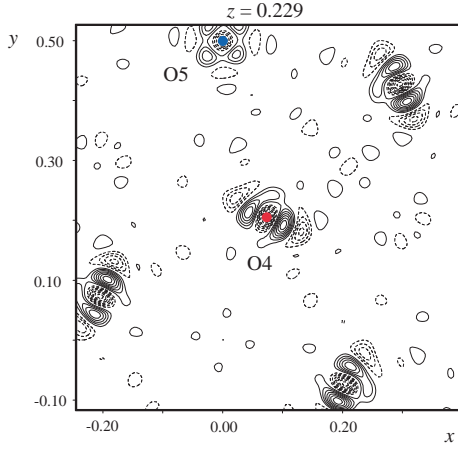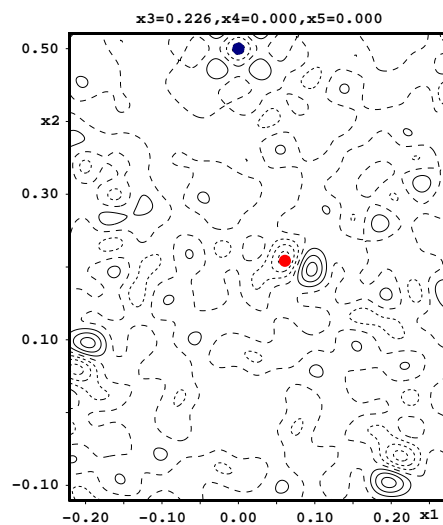

Figure 2: Difference Fourier map of the refined average structure of SNB61 at ambient temperature at $z = 0.229$ showing the atoms O4 (center, red color online) (0.0767,0.2049,0.229) and O5 (top left, blue color online) $(0,\frac{1}{2},0.231)$ (circles). Contours 1 , maximum 8.2, minimum -8.2 (fm/ $Å^3$).

Figure 3: Difference Fourier map of the refined modulated structure of SNB61 (dataset 1) at ambient temperature at $z = 0.225$ showing the atoms O4 (center, red online version) and O5 (top, blue online version). Contours maximum 7.3, minimum -7.6, in steps of 2 (fm/ Å^3).

11

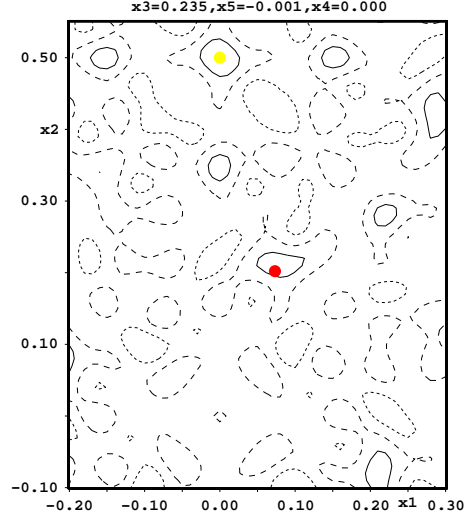Figure 4: Difference Fourier map of the refined modulated structure of SNB34 (dataset 2) at ambient temperature at $z = 0.234$ showing the atoms O4 (center, red online version) and O5 (top, yellow online version). Contours 1 , maximum 2.0, minimum -1.9.
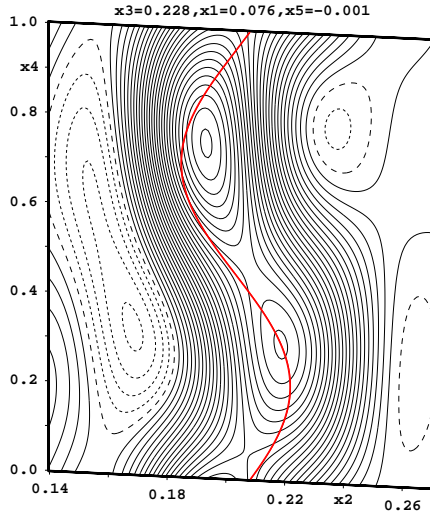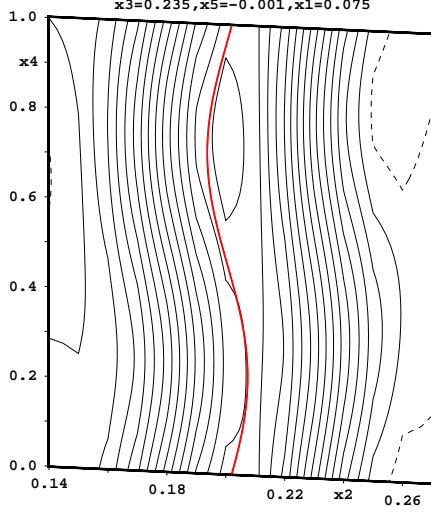

Figure 5: Observed positional modulation of Oxygen atom O4 of SBN61 at ambient temperature. Lines (color online) are fitted atomic positions. The contours are from -8.5 to 56.4 in steps of 2 (fm/ Å^3).

12

Figure 6: Observed positional modulation of Oxygen atom O4 of SBN34 at ambient temperature. Lines (color online) are fitted atomic positions. The contours are from -1.4 to 31.4 in steps of 2 (fm/ $Å^3$).
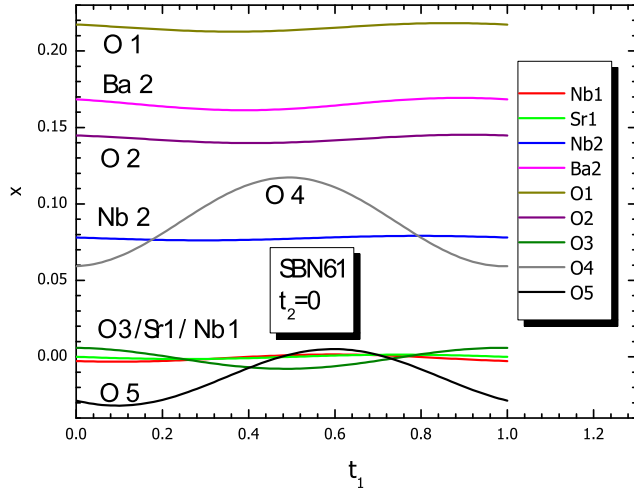

Figure 7: Modulations of x component from the atoms Nb1, Nb2, Sr1, Ba2, and 01-O5 in SBN61 along t_1 at t_2=0.
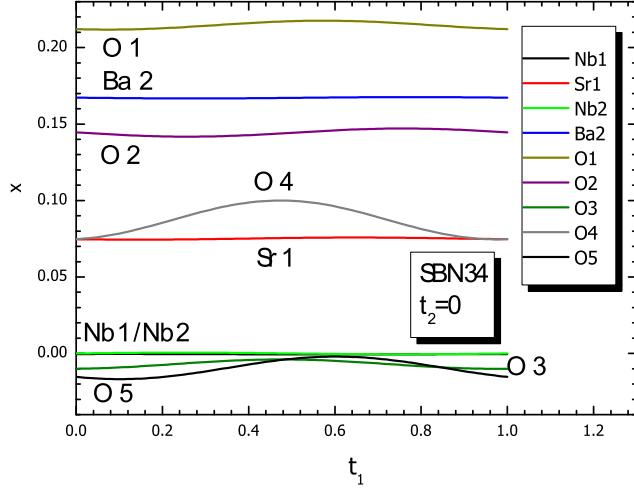
13

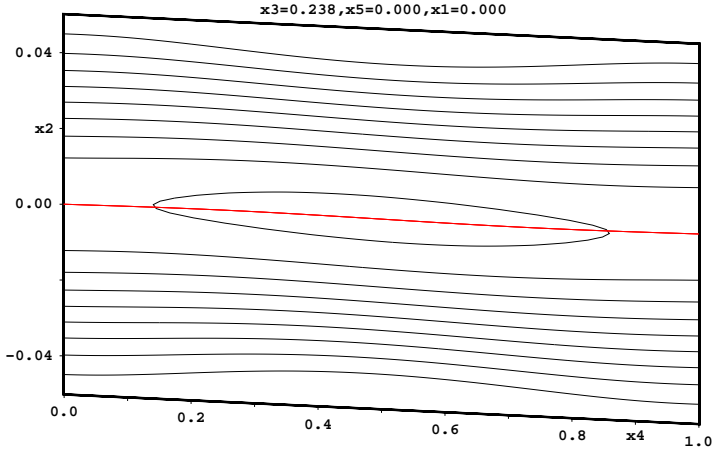Figure 8: Modulations of x component from the atoms Nb1, Nb2, Sr1, Ba2, and 01-O5 in SBN34 along t_1 at t_2=0.

Figure 9: Observed Fourier map in the x2/x4 plane at ambient temperature through the center of the Sr1 atom, showing the absence of any modulation for the Strontium atom Sr1. The bold horizontal line (red color online) is the fitted atomic position of Sr1. The contours are from -1.36 to 18.53 in steps of 2 (fm/ Å^3).
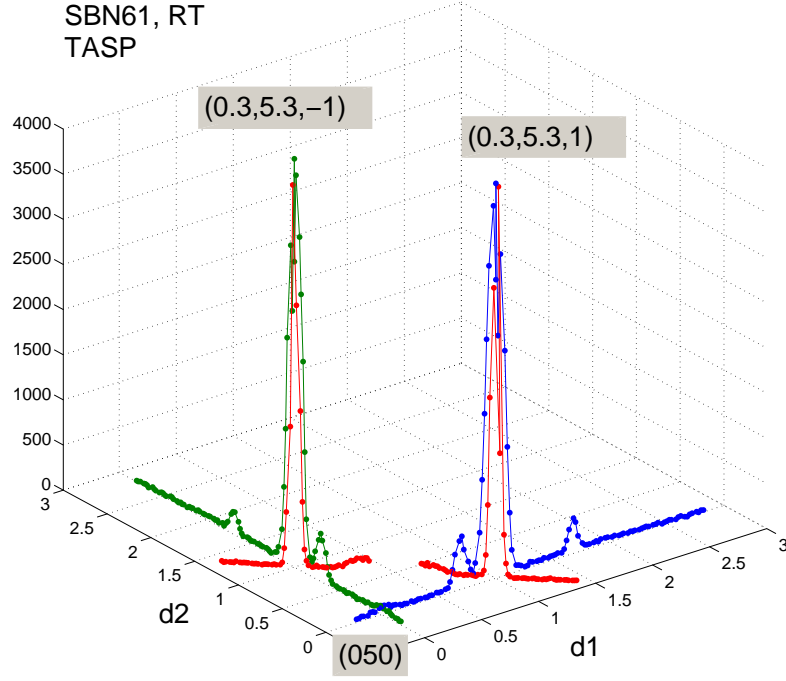
14

Figure 10: Q-scans of SBN61 in a plane formed by the (050) reflection and the two reciprocal vectors $\mathbf{d_1}$=(.3075,.3075,1) and $\mathbf{d_2}$=(.3075,.3075,-1) with respect to the double c-axis as given in table 1. Measurement performed on TASP/SINQ with (λ=2.3603Å) at ambient temperature. Side reflections of the satellites correspond to (002)- and (111)-aluminum-powder lines from holder of the crystal, crossed by the 2 scans along $\mathbf{d_1}$ (color online: blue) and $\mathbf{d_2}$ (color online: green) and the (111)-Al line touched by the scan along $\mathbf{d_2}$-$\mathbf{d_1}$(color online: red)

Table 1: Experimental data collection parameters for $Sr_xBa_{1-x}Nb_2O_6$, SBN61 (x=.61) and SBN34 (x=.34), at ambient temperature. The detailed results are listed in a separated appendix [27].

	5C2/LLB	TriCS/SINQ
	SBN61	SBN34
Dataset	1	2
space group	$P4bm(\alpha,\alpha,\frac{1}{2},\alpha-\alpha,\frac{1}{2})$	$P4bm(\alpha,\alpha,\frac{1}{2},\alpha-\alpha,\frac{1}{2})$
Z	10	10
Radiation	n	n
wavelength λ (Å)	0.835(1)	1.1800(13)
T (K)	300	300
a=b (Å)	12.4815(3)	12.4968 (30)
$c = 2 \cdot c_{av}$ (Å)	7.8856(2)	7.9604(20)
$\mathbf{Q_{1,2}}=\alpha\cdot(\mathbf{a^*}\pm\mathbf{b^*})$, $\alpha=$	0.3075	0.2958
V (Å^3)	1228.5	1243.2
d (g/cm^3)	5.256	5.371
$[\sin(\theta)/\lambda]_{max}$ (Å^{-1})	1.00	0.694
abs. coeff. (mm^{-1})	0.001	0.0018
T^{**}_{min}	0.9944	0.9866
T^{**}_{max}	0.9953	0.9881
crystal dimensions $a \cdot b \cdot c$ (mm^3)	$4 \cdot 4 \cdot 5$	$8.7 \cdot 8.5 \cdot 8.92$
Polarisation [V/mm], Temperature [degC]	270, 130	not poled
crystal volume (mm^3)	80	457
h_{max}	24	14
k_{max}	17	15
l_{max}	15	9
m_{max}	1	1
n_{max}	1	1
no. of refined reflections	5256	1236
no. of obs. reflections (I>3σ)	2527	3620
no. of obs. main reflections (I>3σ)	1220	459
no. of obs. first order satellite reflections (I>3σ)	1307	777
no. of obs. second order satellite reflections (I>3σ)	0	-
no. of measured second order satellite reflections	829	-
$R^{\dagger}_{int}$	0.0285	0.015
$g^{\ddagger}_{iso}$ (10^{-4})	0.092	.005
Refinement[1]		
S	7.39	6.96
R_{obs},R_{all}	11.56	9.06
$R_{w,obs}$,$R_{w,all}$	9.08	11.16
main reflections		
R_{obs}, R_{all}	5.79	7.15
$R_{w,obs}$, $R_{w,all}$	6.38	10.39
satellites of order 1		
R_{obs},R_{all}	21.24	13.86
$R_{w,obs}$, $R_{w,all}$	19.23	13.46

**transmission factors, *i.e.* minimal and maximal amount of transmitted neutrons

†*R-factors* of merging process; ‡Isotropic extinction correction of type I (Lorentzian distriution) is used [30, 31, 32].

[1]: refinement using isotropic temperature factors, all agreement factors in [%].

Table 2: Atomic Fourier amplitudes of selected atoms in SBN61/LLB (dataset 1) and SBN34/TriCS (dataset 3) at ambient temperature of the displacive modulation functions (details of the formalism are given in Eq. 3.24 in [36]. The full table is given in an appendix [27]. Wave symbol c correspond to a cosinus, s to a sinus modulation, 1 and 2 to modulation vectors $\mathbf{Q_{1,2}}$)

atom	wave	x	y	z	x	y	z
		SBN61, 5C2, dataset 1			SBN34, TriCS, dataset 2		
Nb1		0	0.5	0.0019(5)	0	0.5	0.0067
	s,1,0	-0.0024(4)	-0.0024(4)	0		0.0001(6)	0.0001(6)
	c,1,0	0	0	-0.0034(10)	0	0	0.0004(10)
	s,0,1	0.0010(5)	-0.0010(5)	0	0.0006(6)	-0.0006(6)	0
	c,0,1	0	0	-0.0017(10)	0	0	-0.0022(10)
Nb2		0.07463(6)	0.21139(6)	-0.0085(4)	0.07397(10)	0.21084(10)	0.0016(6)
	s,1,0	-0.0010(4)	-0.0013(4)	-0.0034(5)	-0.007(5)	0.0016(5)	-0.0002(5)
	c,1,0	0.0011(4)	0.0016(4)	-0.0024(5)	-0.0007(5)	0.0016(5)	-0.0002(5)
	s,0,1	-0.0039(4)	0.0024(4)	-0.0019(5)	-0.0001(5)	0.0010(4)	0.0002(5)
	c,0,1	0.0021(4)	-0.0021(4)	0.0004(5)	-0.0003(4)	0.0019(4)	-0.0003(5)
Sr1		0	0	0.2368(5)	0	0	0.2426(10)
	s,1,0	-0.0014(6)	0.0003(6)	0	0.0005(6)	0.0026(6)	0
	c,1,0	0	0	-0.0026(10)	0	0	-0.0134(14)
	s,0,1	0.0003(6)	0.0014(6)	0	0.0026(6)	-0.0005(6)	0
	c,0,1	0	0	-0.0026(10)	0	0	-0.0134(14)
Ba1		0.17215(11)	0.67215(11)	0.241	0.1729	0.6729	0.2461
	s,1,0	0.0032(5)	0.0032(5)	-0.0030(14)	0.0001(4)	0.0001(4)	0.0019(14)
	c,1,0	0.0024(6)	0.0024(6)	0.0081(12)	0.0004(4)	0.0004(4)	0.0027(15)
	s,0,1	0.0057(10)	-0.0057(10)	0	0.0060(5)	-0.0060(5)	0
	c,0,1	-0.0038(6)	-0.0038(6)	0.0011(15)	-0.0016(4)	-0.0016(4)	0.0003(14)
Sr2		0.1721	0.6721	0.241	0.17295(16)	0.67295(16)	0.2461(11)
	s,1,0	0.0032(5)	0.0032(5)	-0.0030(14)	0.0001(4)	0.0001(4)	0.0019(14)
	c,1,0	0.0024(6)	0.0024(6)	0.0081(12)	0.0004(4)	0.0004(4)	0.0027(15)
	s,0,1	0.0057(10)	-0.0057(10)	0	0.0060(5)	-0.0060(5)	0
	c,0,1	-0.0038(6)	-0.0038(6)	0.0011(15)	-0.0016(4)	-0.0016(4)	0.0003(14)
O1		0.21835(10)	0.28165(10)	-0.0214(6)	0.21663(14)	0.28337(14)	-0.0143(9)
	s,1,0	0.0003(7)	0.0003(7)	0	-0.0029(6)	-0.0029(6)	0
	c,1,0	0.0028(8)	-0.0028(8)	0.0186(9)	-0.0005(7)	0.0005(7)	0.0111(8)
	s,0,1	-0.0024(7)	0.0024(7)	0.0099(10)	-0.0009(6)	0.0009(6)	0.0091(8)
	c,0,1	-0.0032(7)	0.0032(7)	-0.0151(10)	-0.0021(7)	0.0021(7)	-0.0074(9)
O2		0.13938(10)	0.06819(9)	-0.0268(6)	0.14047(15)	0.06960(13)	-0.0209(8)
	s,1,0	-0.0005(8)	-0.0023(7)	0.0220(8)	-0.0024(7)	0.0010(7)	0.0105(6)
	c,1,0	0.0027(8)	-0.0053(7)	0.0170(10)	0.0011(7)	0.0016(7)	0.0085(7)
	s,0,1	-0.0055(8)	-0.0034(8)	0.0157(9)	0.0034(7)	-0.0006(6)	0.0081(6)
	c,0,1	0.0039(8)	-0.0036(7)	-0.0237(8)	0.0035(7)	0.0015(7)	-0.0163(6)
O3		-0.00585(10)	0.34357(9)	-0.0280(6)	-0.00618(15)	0.34372(15)	-0.0186(9)
	s,1,0	0.0037(7)	0.0041(6)	-0.0291(6)	-0.0014(7)	-0.0055(6)	-0.0127(6)
	c,1,0	0.0058(8)	0.0017(8)	-0.0093(10)	-0.0027(7)	0.0012(7)	-0.0041(7)
	s,0,1	-0.0041(6)	-0.0052(5)	-0.0256(8)	0.0026(7)	0.0009(6)	-0.0184(7)
	c,0,1	0.0030(9)	-0.0008(8)	0.0094(11)	0.0009(7)	-0.0013(7)	0.0050(6)
O4		0.07605(18)	0.20492(15)	0.2275(5)	0.0749(2)	0.20557(19)	0.2351(9)
	s,1,0	-0.0137(6)	0.0178(3)	0.0041(6)	-0.0044(5)	0.0067(4)	-0.0086(10)
	c,1,0	-0.0256(4)	0.0050(4)	-0.0062(5)	-0.0119(5)	0.0014(4)	-0.0032(10)
	s,0,1	-0.0087(7)	0.0016(6)	0.0091(8)	-0.0107(5)	0.0056(4)	-0.0069(9)
	c,0,1	0.0104(6)	-0.0014(6)	-0.0024(9)	0.0101(5)	-0.0049(4)	0.0017(11)
O5		0	0.5	0.2301(6)	0	0.5	0.2347(11)
	s,1,0	-0.0185(6)	-0.0185(6)	0	-0.0074(6)	-0.0074(6)	0
	c,1,0	0	0	0.002(2)	0	0	-0.002(2)
	s,0,1	0.0163(4)	-0.0163(4)	0	0.0117(6)	-0.0117(6)	0
	c,0,1	0	0	-0.0124(16)	0	0	-0.001(2)

Table 3: Symmetry codes used in JANA2000.

(i)	$x1$	$x2$	$x3$	$x5$	$-x4$
(iii)	$\frac{1}{2} - x1$	$\frac{1}{2} + x2$	$x3$	$-x5$	$-x4$
(iv)	$-x1$	$-x2$	$x3$	$-x4$	$-x5$
(v)	$\frac{1}{2} - x2$	$\frac{1}{2}$-x1	$x3$	$-x4$	$x5$
(vi)	$x2$	$-x1$	$x3$	$-x5$	$x4$
(vii)	$\frac{1}{2} + x1$	$\frac{1}{2} - x2$	$x3$	$x5$	$x4$
(viii)	$\frac{1}{2} + x2$	$\frac{1}{2} + x1$	$x3$	$x4$	$-x5$

Table 4: Comparison of selected interatomic distances in the NbO_6-octahedra for SBN61 (neutron and X-ray data) and SBN34 (neutron data only). O4 and O5 are interchanged in this study and in the X-ray study of Woike et al. [19]. All distances are in [Å].

sample	SBN61		SBN61		SBN 34	
dataset	1/neutron		Xray/Woike [19]		2/neutron	
	dmin	dmax	dmin	dmax	dmin	dmax
Nb2-O4	1.721(14)	2.029(15)	1.79(3)	1.98(3)	1.746(19)	2.010(19)
Nb2-O4^{iv}	1.959(14)	2.213(15)	1.95(3)	2.18(3)	2.022(19)	2.280(19)